

$B_s \rightarrow \mu^+ \mu^- \gamma$ and $B_s \rightarrow \phi \gamma$
decay rates from $N_f = 2 + 1 + 1$
twisted mass simulations



Based on:

"The $B_s \rightarrow \mu^+ \mu^- \gamma$ decay rate at large q^2 from lattice QCD"

R.Frezzotti G. Gagliardi, V. Lubicz, G. Martinelli, C.T. Sachrajda,
F. S, S. Simula, N. Tantalo [Phys.Rev.D 109 (2024)]



Francesco Sanfilippo, INFN Roma Tre
Lattice 2024, 30 July 2024



$B_s \rightarrow \mu^+ \mu^- \gamma$ at large q^2 , why?

- **NOVELTY:** New test of the SM predictions in the $b \rightarrow s$ FCNC transitions
- **SENSITIVITY:** more Wilson coefficients involved, larger set than $B_s \rightarrow \mu^+ \mu^-$
- **OPPORTUNITY:** Yes, it is suppressed by $\mathcal{O}(\alpha_{em})$ w.r.t $B_s \rightarrow \mu^+ \mu^-$ due to extra photon emission, but!, it is helicity anti-suppressed, so the two are similar in magnitude, target of LHCb analysis – prediction, not postdiction!
- **CLEANNESS:** provided that $\sqrt{q^2}$ = invariant mass of $\mu^+ \mu^-$ is large enough, the contribution from penguin operator (highly challenging) are suppressed.
[Guadagnoli, Reboud, Zwicky, JHEP '17]

Here: $\sqrt{q^2} > 4.2$ GeV

The decay in the Weak Hamiltonian

Full Weak Hamiltonian for $b \rightarrow s$ processes:

$$\mathcal{H}_{\text{eff}}^{b \rightarrow s} = 2\sqrt{2}G_F V_{tb}V_{ts}^* \left[\sum_{i=1,2} C_i(\mu) \mathcal{O}_i^c + \sum_{i=3}^6 C_i(\mu) \mathcal{O}_i + \frac{\alpha_{\text{em}}}{4\pi} \sum_{i=7}^{10} C_i(\mu) \mathcal{O}_i \right]$$

current-current: $\mathcal{O}_1^c = (\bar{s}_i \gamma^\mu P_L c_j) (\bar{c}_j \gamma^\mu P_L b_i)$, $\mathcal{O}_2^c = (\bar{s} \gamma^\mu P_L c) (\bar{c} \gamma^\mu P_L b)$

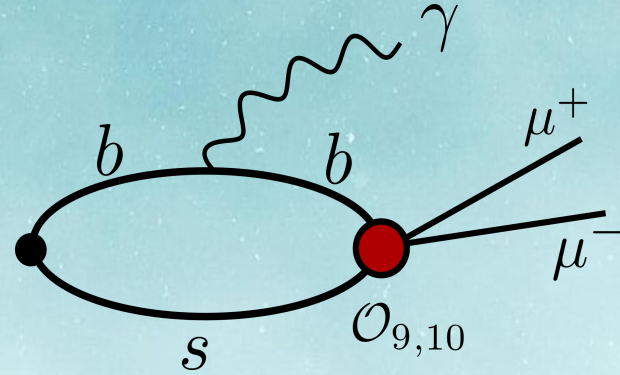
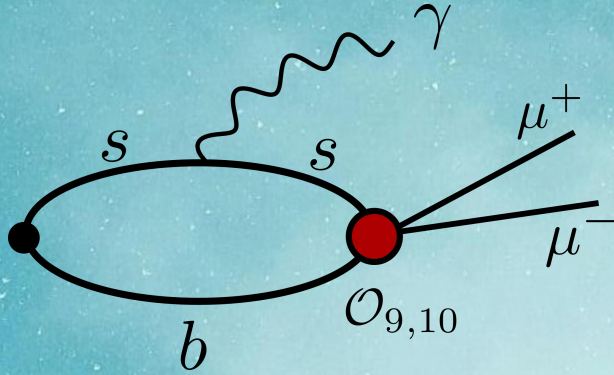
ph./chromo. penguins: $\mathcal{O}_7 = -\frac{m_b}{e} \bar{s} \sigma^{\mu\nu} F_{\mu\nu} P_R b$, $\mathcal{O}_8 = -\frac{g_s m_b}{4\pi \alpha_{\text{em}}} \bar{s} \sigma^{\mu\nu} G_{\mu\nu} P_R b$

semileptonic: $\mathcal{O}_9 = (\bar{s} \gamma^\mu P_L b) (\bar{\mu} \gamma_\mu \mu)$, $\mathcal{O}_{10} = (\bar{s} \gamma^\mu P_L b) (\bar{\mu} \gamma_\mu \gamma^5 \mu)$

To lowest order in $\mathcal{O}(\alpha_{em})$:

$$\mathcal{A}[\bar{B}_s \rightarrow \mu^+ \mu^- \gamma] = -e \frac{\alpha_{\text{em}}}{\sqrt{2}\pi} V_{tb}V_{ts}^* \varepsilon_\mu^* \left[\sum_{i=1}^9 C_i \overbrace{H_i^{\mu\nu}}^{\text{NP-QCD}} L_{V\nu} + C_{10} \left(\overbrace{H_{10}^{\mu\nu}}^{\text{NP-QCD}} L_{A\nu} - \overbrace{\frac{i}{2} f_{B_s} L_A^{\mu\nu} p_\nu}^{\text{PT-contribution}} \right) \right]$$

Semileptonic operators contribution

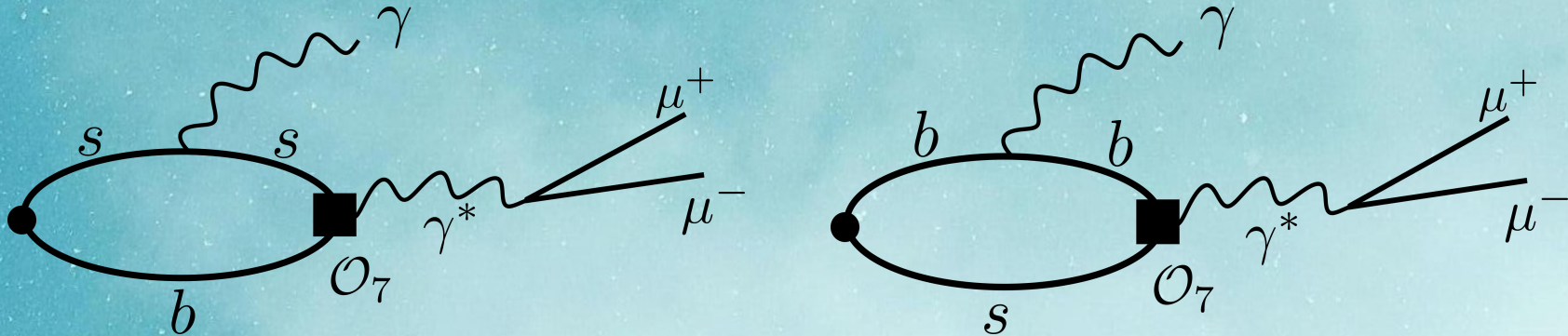


$$\begin{aligned}
 H_9^{\mu\nu}(p, k) &= H_{10}^{\mu\nu}(p, k) = i \int d^4y e^{iky} \hat{T} \langle 0 | [\bar{s} \gamma^\nu P_L b](0) J_{\text{em}}^\mu(y) | \bar{B}_s(p) \rangle \\
 &= -i [g^{\mu\nu} (k \cdot q) - q^\mu k^\nu] \frac{F_A}{2m_{B_s}} + \varepsilon^{\mu\nu\rho\sigma} k_\rho q_\sigma \frac{F_V}{2m_{B_s}}
 \end{aligned}$$

Two form factors: $F_V(x_\gamma)$ and $F_A(x_\gamma)$ with $x_\gamma = 2E_\gamma/m_{B_s}$ photon energy in units of $2B_s$ mass

“Bread and butter” lattice techniques (so to say)

A-Type penguin operators

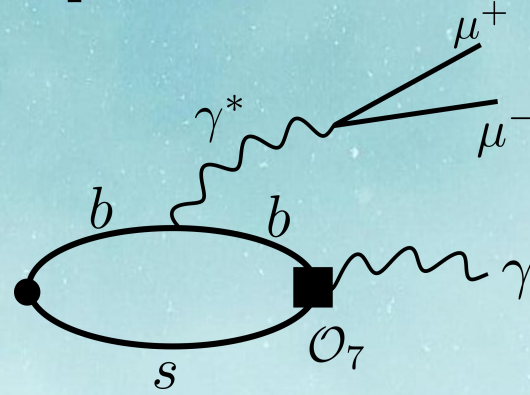
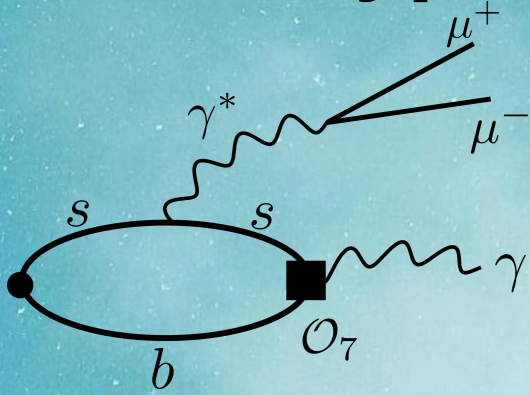


$$\begin{aligned}
 H_{7A}^{\mu\nu}(p, k) &= i \frac{2m_b}{q^2} \int d^4y e^{iky} \hat{T} \langle 0 | [-i\bar{s}\sigma^{\nu\rho}q_\rho P_R b] (0) J_{\text{em}}^\mu(y) | \bar{B}_s(p) \rangle \\
 &= -i [g^{\mu\nu}(k \cdot q) - q^\mu k^\nu] \frac{\bar{F}_T m_b}{q^2} + \varepsilon^{\mu\nu\rho\sigma} k_\rho q_\sigma \frac{\bar{F}_T m_b}{q^2}
 \end{aligned}$$

Tensor-axial $F_{TA}(x_\gamma)$ and tensor-vector $F_{TV}(x_\gamma)$ form factors

Similar, but needs to explicitly renormalized via Z_T

B-Type penguin operators



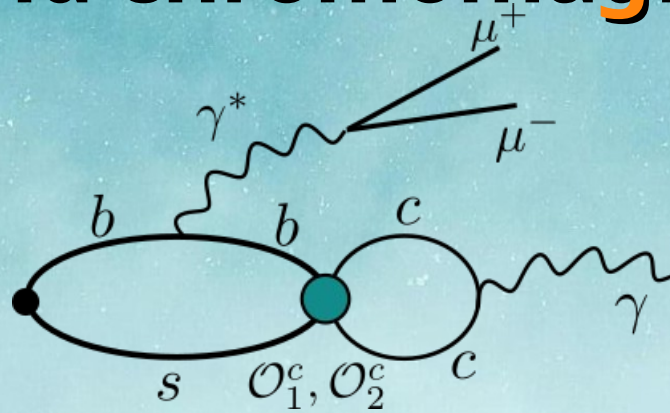
$$\begin{aligned}
 H_{7B}^{\mu\nu}(p, k) &= i \frac{2m_b}{q^2} \int d^4y e^{iqy} \hat{T} \langle 0 | [-i\bar{s}\sigma^{\mu\rho}k_\rho P_R b] (0) J_{\text{em}}^\nu(y) | \bar{B}_s(p) \rangle \\
 &= -i [g^{\mu\nu}(k \cdot q) - q^\mu k^\nu] \frac{\bar{F}_T m_b}{q^2} + \varepsilon^{\mu\nu\rho\sigma} k_\rho q_\sigma \frac{\bar{F}_T m_b}{q^2}
 \end{aligned}$$

Computing $\bar{F}_T(x_\gamma)$ is challenging!, ought to the nontrivial analytic continuation from euclidean

Evaluated via novel spectral density methods - [Frezzotti et al, PRD 108 '23]

Negligible contribution within current accuracy.

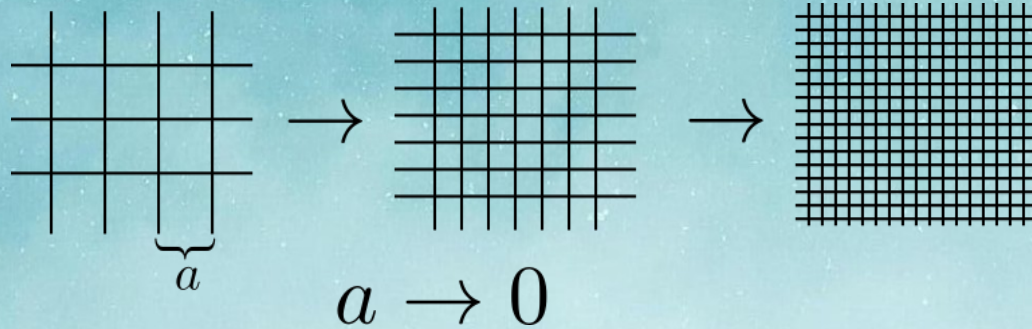
Four-quarks and chromomagnetic operators



$$H_{i=1-6,8}^{\mu\nu}(p, k) = \frac{(4\pi)^2}{q^2} \int d^4y d^4x e^{iky} e^{iqx} \hat{T} \langle 0 | J_{\text{em}}^\mu(y) J_{\text{em}}^\nu(x) \mathcal{O}_i(0) | \bar{B}_s(p) \rangle$$

- In high q^2 region: formally of higher-order in $1/m_b$ expansion [Guadagnoli, Reboud, Zwicky, JHEP17]
- We did not compute them, but have developed a strategy to be studied in the near future
- We included a phenomenological description of the supposed dominant contribution (depicted).

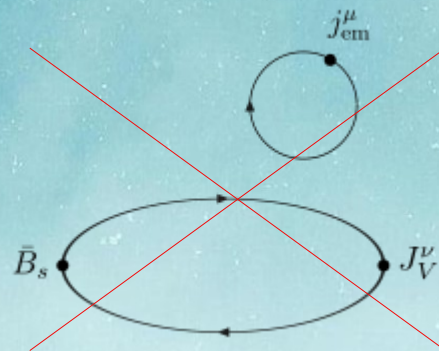
Continuum limit extrapolation



- Four ensembles of ETM collaboration $N_f = 2 + 1 + 1$ ensembles,
- Lattice spacing in the range $a \in [0.057 : 0.09]$ fm
- Three out four are at M_π^{phys} (for what it matters here...)
- Limit $a \rightarrow 0$ carried out at fixed heavy meson mass and kinematic, to ease the extrapolation
- Five heavy meson masses $M_{H_s} \in [M_{D_s} : 2M_{D_s}]$
- Physical M_{B_s} achieved extrapolating via pole-like+HQET scaling relation

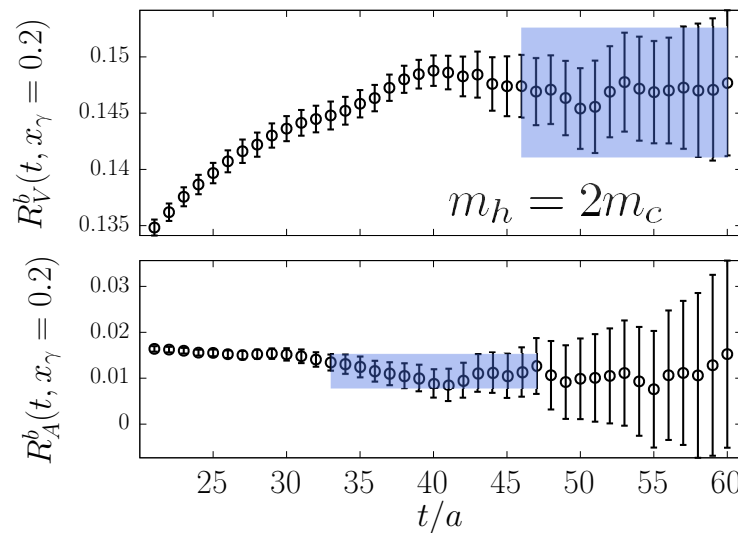
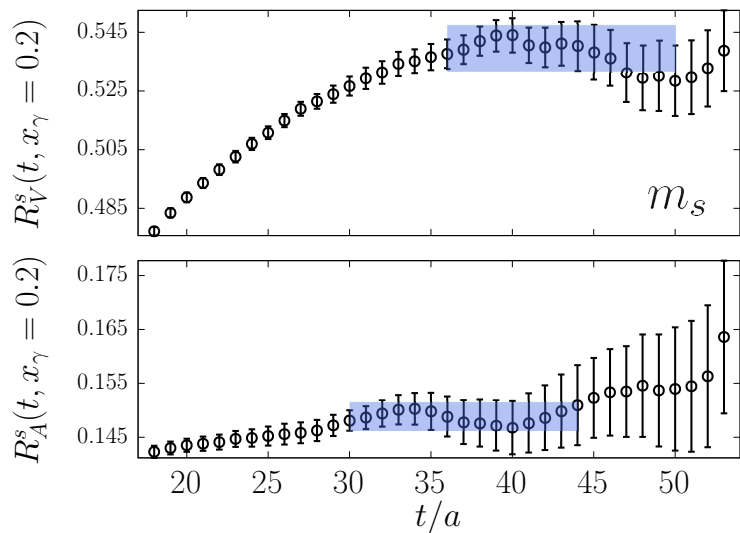


Electroquenched approximation



Vanishing
in the
 $SU(3)$
symmetric
limit

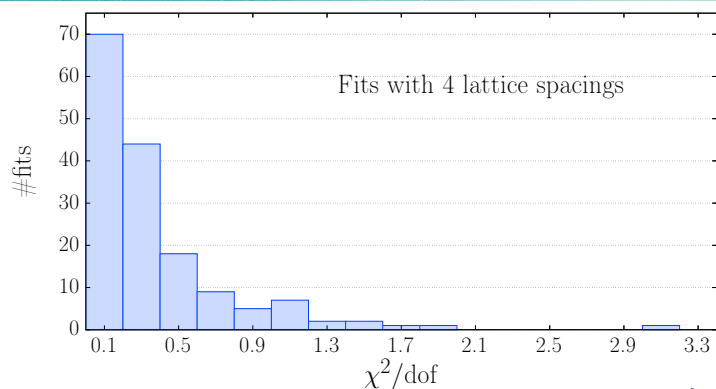
A few plateaus



Strange and heavy
contributions analysed
separately, as they
have different excited
states contributions

Taking the continuum limit

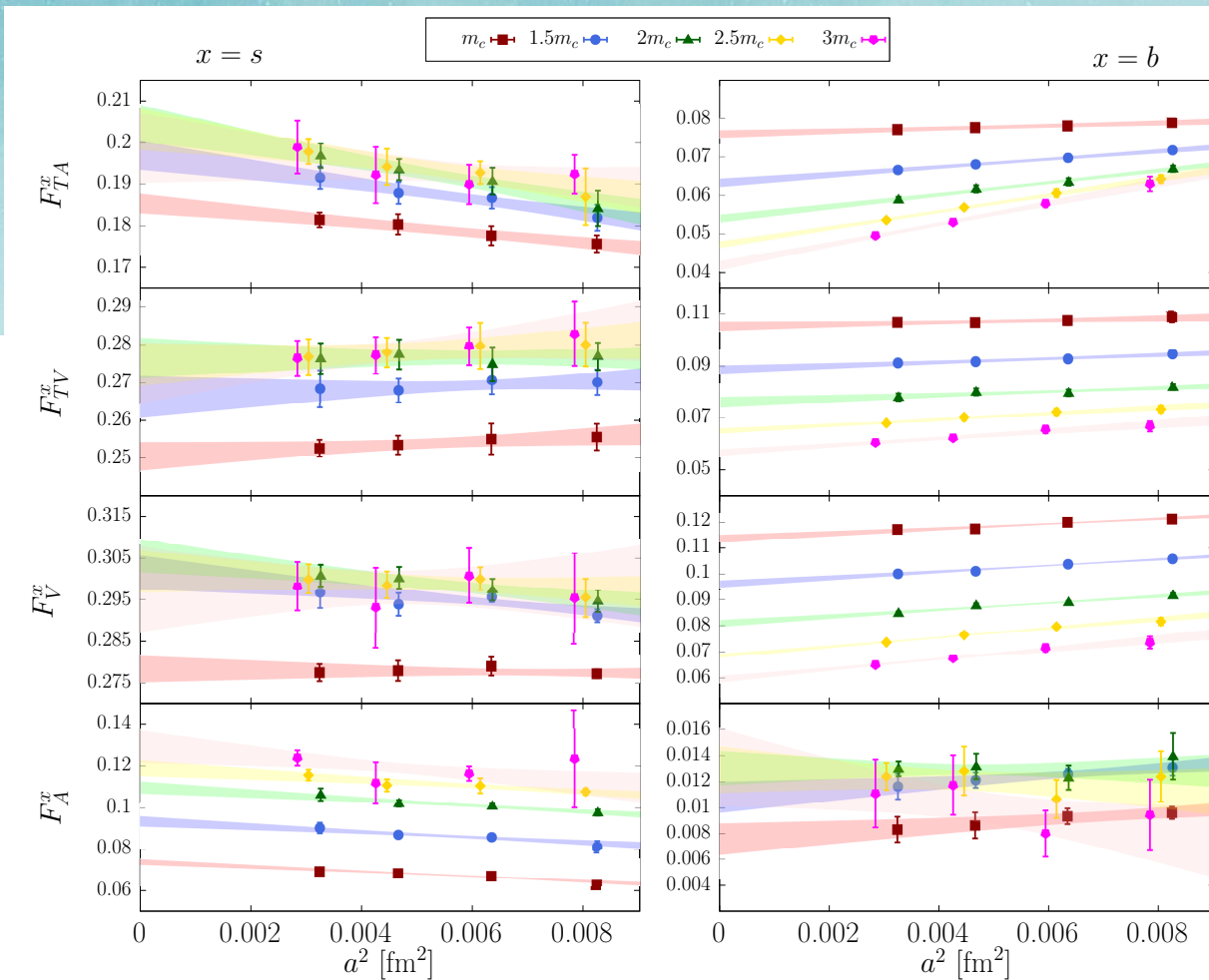
We carried out 160 variations of the continuum limit extrapolation:



Here is an example showing:

$$F_A, F_V, F_{TA}, F_{TV}$$

for the 5 masses at $x_\gamma = 0.4$



Extrapolating to the physical M_{B_s}

Heavy-mass/large-energy EFT [Beneke et al, EPJC 2011, JHEP 2020] predicts:

$$\frac{F_W(x_\gamma, m_{H_s})}{f_{H_s}} \propto \frac{|q_s|}{x_\gamma} + \mathcal{O}\left(\frac{1}{E_\gamma}, \frac{1}{m_{H_s}}\right) \quad W = \{V, A, TV, TA\}$$

but resonance contributions are to be expected, we include them relying on VMD

$$\begin{aligned} \frac{F_V(x_\gamma, z)}{f_{H_s}} &= \frac{|q_s|}{x_\gamma} \frac{1}{1 + C_V \frac{2z^2}{x_\gamma}} [K + \text{NLO} + \text{NNLO}] \\ \frac{F_A(x_\gamma, z)}{f_{H_s}} &= \frac{|q_s|}{x_\gamma} \frac{1}{1 + C_A \frac{2z}{x_\gamma}} [K + \text{NLO} + \text{NNLO}] \\ \frac{F_{TV}(x_\gamma, z)}{f_{H_s}} &= \frac{|q_s|}{x_\gamma} \frac{1 + 2C_V z^2}{1 + C_V \frac{2z^2}{x_\gamma}} [K_T + \text{NLO} + \text{NNLO}] \\ \frac{F_{TA}(x_\gamma, z)}{f_{H_s}} &= \frac{|q_s|}{x_\gamma} \frac{1 + 2C_A z}{1 + C_A \frac{2z}{x_\gamma}} [K_T + \text{NLO} + \text{NNLO}] \end{aligned}$$

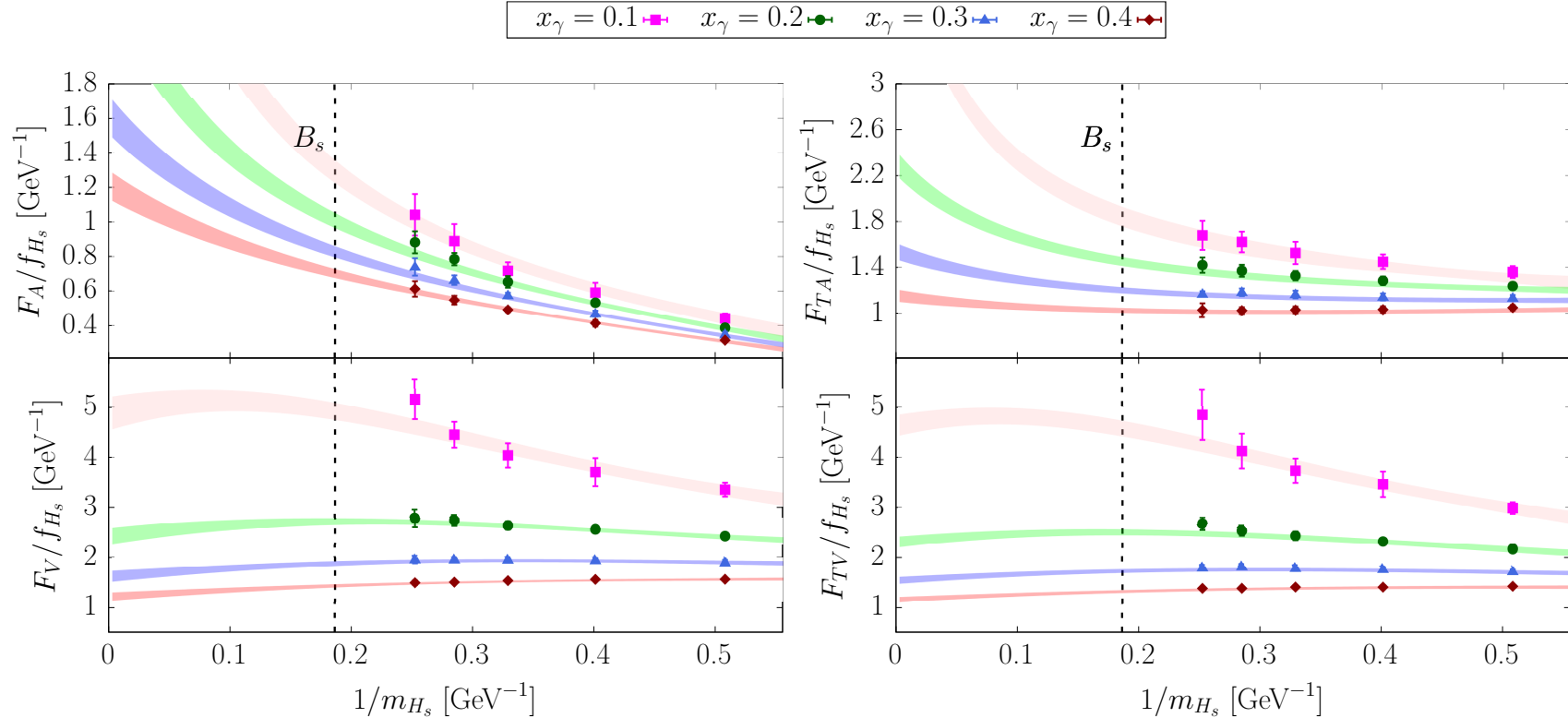
$C_{V(A)}$ related to the mass splitting of vector(axial) vs. pseudoscalar meson

NLO in terms of $1/E_\gamma$, $1/M_{H_s}$

NNLO in terms of $1/E_\gamma^2$, $1/M_{H_s}^2$

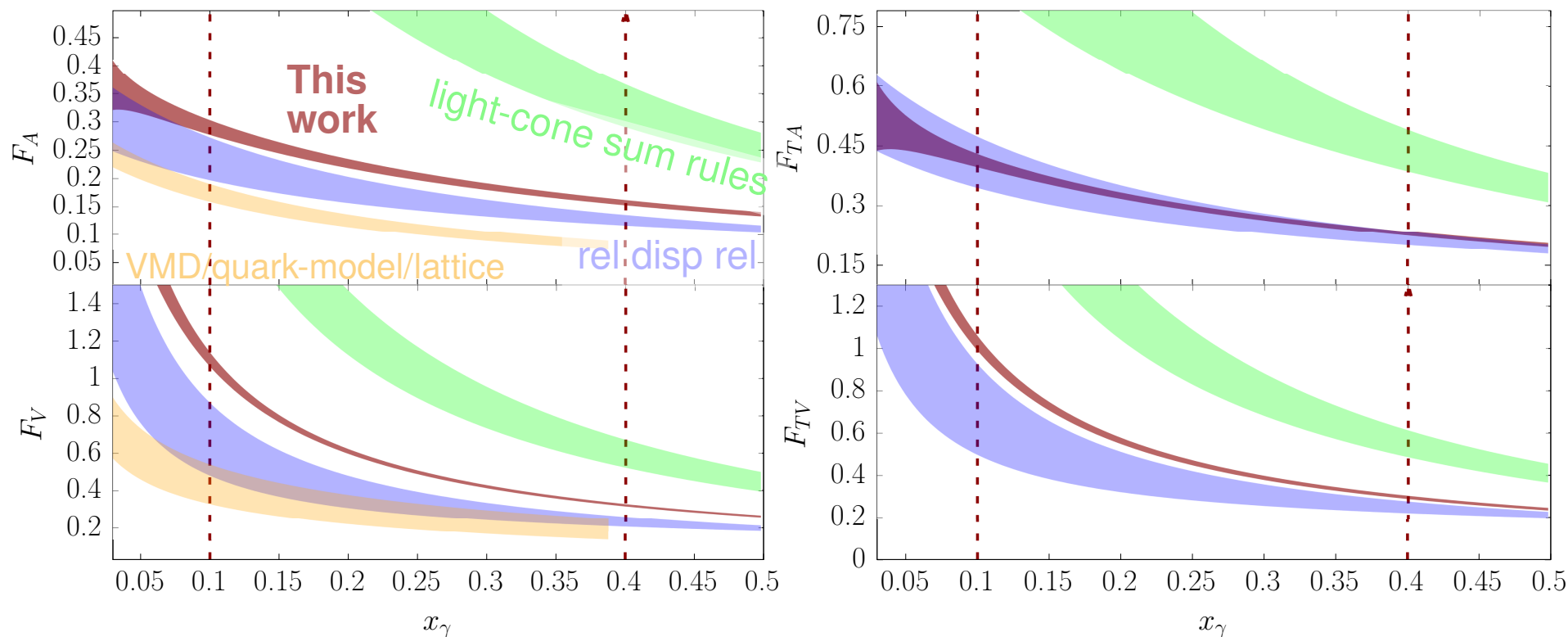
not needed for a good fit, probe the systematic errors

Extrapolations to the physical M_{B_s}



- Heavy meson mass dependence is steeper at small photon energies, as expected
- 500 fits carried out in total, varying NLO and NNLO parameters
- AIC or uniform average with cut at $\chi^2/ndof$ to combine them

Comparison with others (previous work)



Kozachuk, Melikhov, Nikitin [PRD '18]

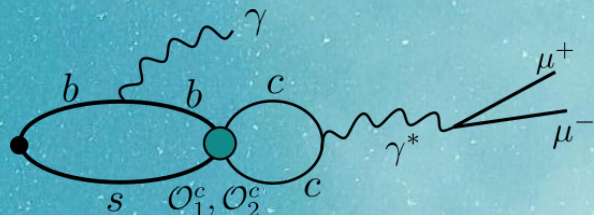
Janowski, Pullin, Zwicky [JHEP '21]

Guadagnoli, Normand, Simula, Vittorio [JHEP '23]

ETM collaboration

Phys.Rev.D 109 (2024)

4-quark operators & chromomagnetic contributions



Expected to be dominated by $J^P = 1^-$ charmonium resonances \mathcal{O}_{1-2}

Interpreted as Wilson coefficient shift $C_9 \rightarrow C_9^{\text{eff}}(q^2) = C_9 - \Delta C_9(q^2)$

We model this contribution using the measured spectrum of vector resonances (as done by [Guadagnoli et al, JHEP '17, '23])

$$\Delta C_9(q^2) = \frac{9\pi}{\alpha_{\text{em}}^2} \bar{C} \sum_V |k_V| e^{i\delta_V} \frac{m_V B(V \rightarrow \mu^+ \mu^-) \Gamma_V}{q^2 - m_V^2 + im_V \Gamma_V}$$

$V_{c\bar{c}}$	$M_{V_{c\bar{c}}}$ [GeV]	Γ [MeV]	$\mathcal{B}(V_{c\bar{c}} \rightarrow \mu^+ \mu^-)$
J/ψ	3.096900(6)	0.0926(17)	0.05961(33)
$\Psi(2S)$	3.68610(6)	0.294(8)	$8.0(6) \cdot 10^{-3}$
$\Psi(3770)$	3.7737(4)	27.2(1.0)	$*9.6(7) \cdot 10^{-6}$
$\Psi(4040)$	4.039(1)	80(10)	$*1.07(16) \cdot 10^{-5}$
$\Psi(4160)$	4.191(5)	70(10)	$*6.9(3.3) \cdot 10^{-6}$
$\Psi(4230)$	4.2225(24)	48(8)	$3.2(2.9) \cdot 10^{-5}$
$\Psi(4415)$	4.421(4)	62(20)	$2(1) \cdot 10^{-5}$
$\Psi(4660)$	4.630(6)	72_{-12}^{+14}	not seen

Other ingredients:

$$\bar{C} = C_1 + C_2/3 \simeq -0.2$$

$\delta_V = |k_V| - 1 = 0$ in factorization approx

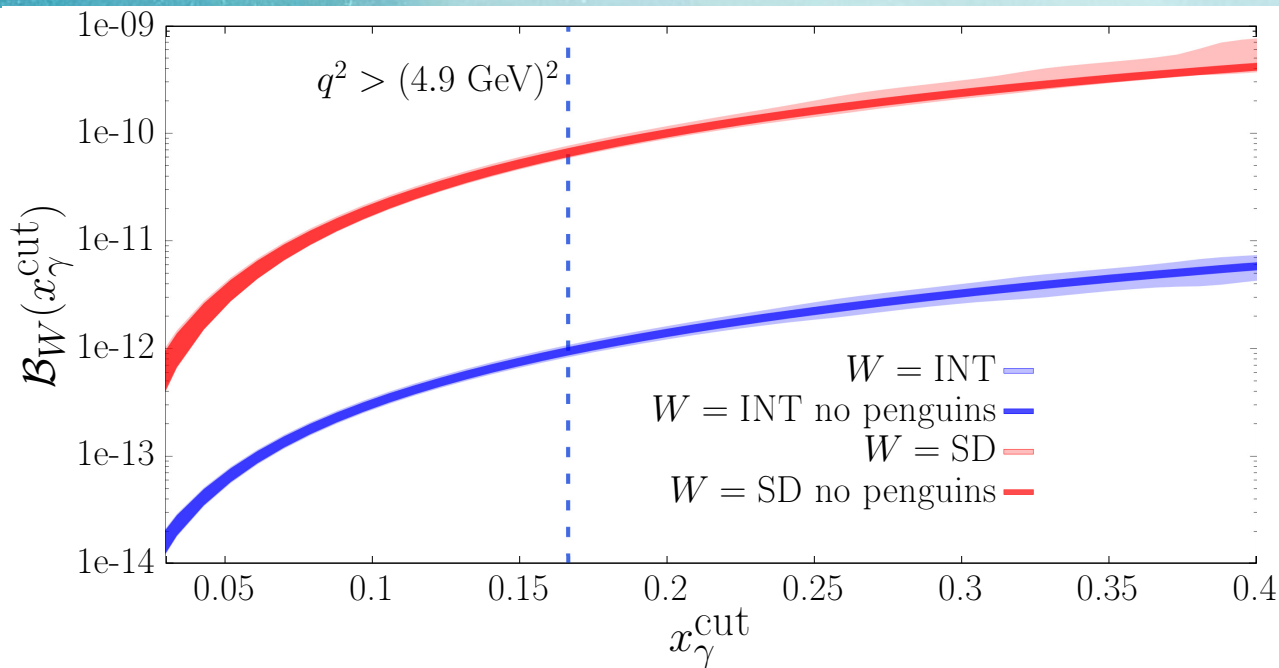
We scan uniformly distributed phases:

$$\delta_V \in [0, 2\pi] \quad \text{and} \quad |k_V| = 1.75(75)$$

Calculation of the branching fraction

$$\mathcal{B}(x_\gamma^{\text{cut}}) = \int_0^{x_\gamma^{\text{cut}}} dx_\gamma \frac{d\mathcal{B}}{dx_\gamma} \quad x_\gamma^{\text{cut}} \equiv 1 - \frac{q_{\text{cut}}^2}{m_{B_s}^2}$$

$E_\gamma^{\text{cut}} = x_\gamma^{\text{cut}} m_{B_s}/2$ is the upper-bound on the measured photon energy



- SD contribution dominated by vector form factor
- Tensor form-factor $F_{TV/A}$ contributions suppressed by small Wilson coefficient $C_7 \ll C_9, C_{10}$
- At $x_\gamma = 0.4$, uncertainties of charming-penguins is $\sim 30\%$

LHCb results presented at Moriond '24

LHCb targets rare radiative decay

Rare radiative b-hadron decays are powerful probes of the Standard Model (SM) sensitive to small deviations caused by potential new physics in virtual loops. One such process is the decay of $B_s^0 \rightarrow \mu^+ \mu^- \gamma$. The dimuon decay of the B_s^0 meson is known to be extremely rare and has been measured with unprecedented precision by LHCb and CMS. While performing this measurement, LHCb also studied the $B_s^0 \rightarrow \mu^+ \mu^- \gamma$ decay, partially reconstructed due to the missing photon, as a background component of the $B_s^0 \rightarrow \mu^+ \mu^-$ process and set the first upper limit on its branching fraction to 2.0×10^{-9} at 95% CL (red arrow in figure 1). However, this search was limited to the high-dimuon-mass region, whereas several theoretical extensions of the SM could manifest

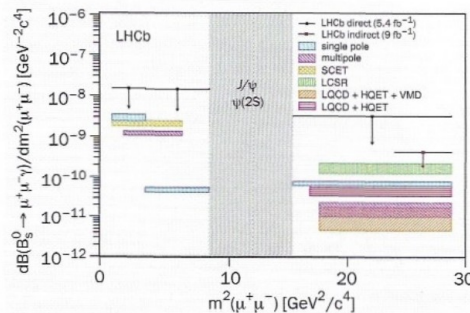


Fig. 1. 95% confidence limits on differential branching fractions for $B_s^0 \rightarrow \mu^+ \mu^- \gamma$ in intervals of dimuon mass squared (q^2). The shaded boxes illustrate SM predictions for the process, according to different calculations.

is performed separately for three dimuon mass ranges to exploit any differences along the spectrum, such as the $\phi(1020)$ meson contribution in the low invariant mass region. The $\mu^+ \mu^- \gamma$ invariant mass distributions of the selected candidates are fitted, including all background contributions and the $B_s^0 \rightarrow \mu^+ \mu^- \gamma$ signal component. Figure 2 shows the fit for the lowest dimuon mass region.

No significant signal of $B_s^0 \rightarrow \mu^+ \mu^- \gamma$ is found in any of the three dimuon mass regions, consistent with the background-only hypothesis. Upper bounds on the branching fraction are set and can be seen as the black arrows in figure 1. The mass fit is also performed for the combined candidates of the three dimuon mass regions to set a combined upper limit on the branching fraction to 2.8×10^{-8} at 95% CL.

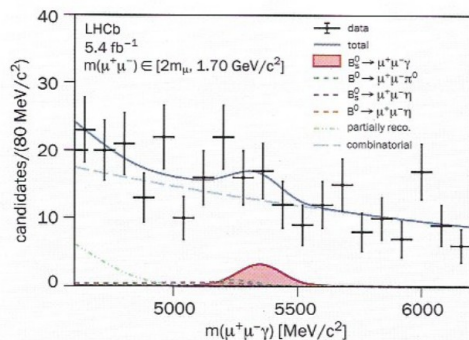


Fig. 2. Mass distribution of $B_s^0 \rightarrow \mu^+ \mu^- \gamma$ candidates for the lowest dimuon mass region, below $1.7 \text{ GeV}/c^2$, with the total fit overlaid (blue line). The signal component (solid red line) is displayed with its total uncertainty (red band). The various background contributions are also displayed.

themselves in lower regions of the dimuon-mass spectrum. Reconstructing the photon is therefore essential to explore the spectrum thoroughly and probe a wide range of physics scenarios.

The LHCb collaboration now reports the first search for the $B_s^0 \rightarrow \mu^+ \mu^- \gamma$ decay with a reconstructed photon, exploring the full dimuon mass spectrum. Photon reconstruction poses additional experimental challenges, such as degrading the mass resolution of the B_s^0 candidate and introducing additional background contributions. To cope with this ambitious search, machine-learning algorithms and new variables have been specifically designed with the aim of discriminating the signal among background processes with similar signatures. The analysis >

The SM theoretical predictions of b decays becomes particularly difficult to calculate when a photon is involved, and they have large uncertainties due to the $B_s^0 \rightarrow \gamma$ local form factors. The $B_s^0 \rightarrow \mu^+ \mu^- \gamma$ decay provides a unique opportunity to validate the different theoretical approaches, which do not agree with each other, as shown by the coloured bands in figure 1. Theoretical calculations of the branching fractions are currently below the experimental limits. The upgraded LHCb detector and the increased luminosity of the LHC's Run 3 is currently providing conditions for studying rare radiative b-hadron decays with greater precision and, eventually, for finding evidence for the $B_s^0 \rightarrow \mu^+ \mu^- \gamma$ decay.

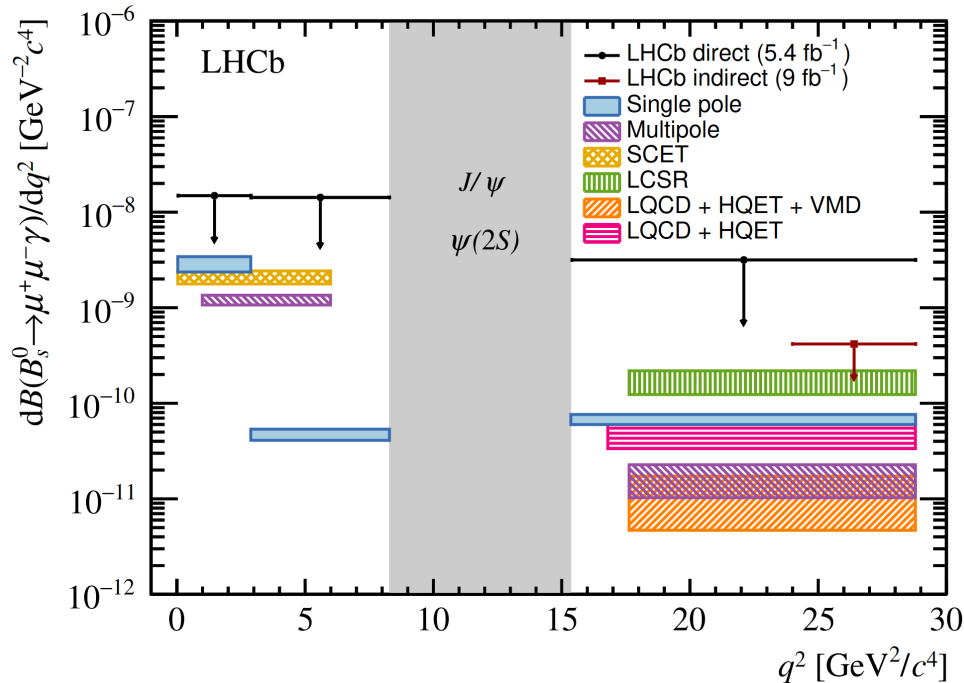
Further reading

LHCb Collab 2024, arXiv:2404.03375.

Comparison with LHCb results

“Search for $B_s^0 \rightarrow \mu^+ \mu^- \gamma$ decay”, LHCb coll, [JHEP 07 (2024) 101]

- LHCb measurement: explicit detection of the photon in the final state
- Upper-bound, for $q_{\text{cut}}^2 \sim 15 \text{ GeV}^2$ roughly one order of magnitude larger than previous bound.



← LHCb [direct method]

← LHCb [indirect method]

← This work

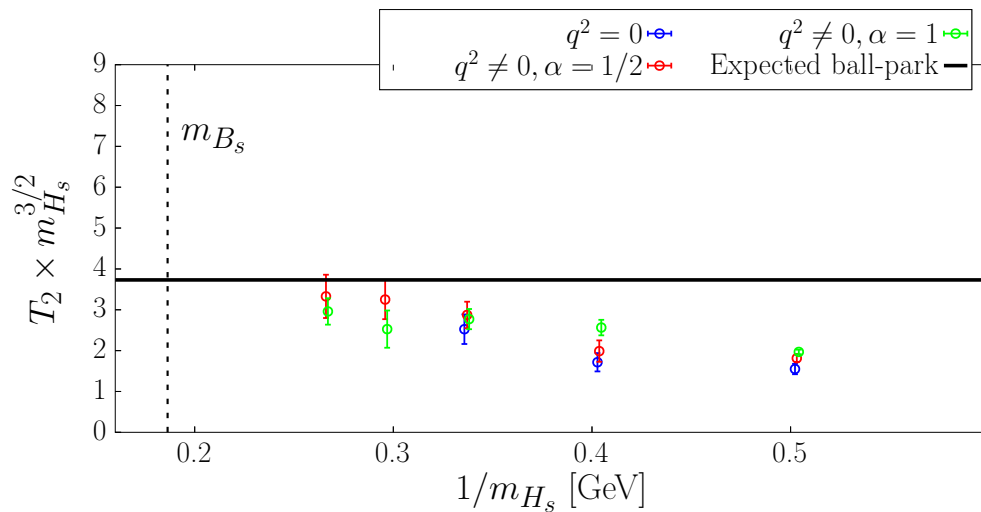
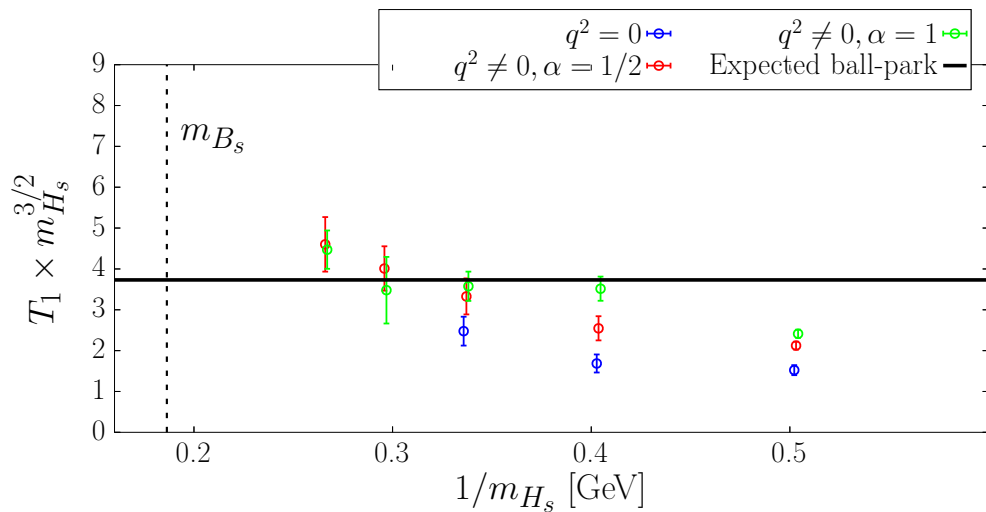
Extension: $B_s \rightarrow \phi\gamma$ decay

- Measured experimentally
- Interesting complementary comparison
- Only a single lattice prediction in the quenched approximation at single lattice spacing

[C. Bernard, P. Hsieh, and A. Soni, Phys. Rev. Lett., 72:1402–1405, 1994]

Work in progress

(“Perhaps we’ll see each other next year in Mumbai”)



Conclusions

Numerically

- Gauge configurations produced by the ETM Collaboration
- Four lattice spacing $a \in [0.057 : 0.09]$ fm
- Five different heavy-strange masses $m_{H_s} \in [m_{D_s} : 2m_{D_s}]$

Results

- First-principles calculation of form factors F_V, F_A, F_{TV}, F_{TA} for $\bar{B}_s \rightarrow \mu^+ \mu^- \gamma$ decay,
- in the electroquenched approximation
- and phenomenologically modelling the dominant charming penguin contributions

Future directions

- **Electro**unquenching, evaluate charming penguins
- Simulate finer lattice spacing to extrapolate from higher heavy meson mass